Symposium Program:

- A Look Back
- Non-redox Flavin Catalyzed Reactions
- Oxygen Activation
- Structure & Coupling Mechanism of Complex I
- Complex Flavoproteins
- Flavin Physics & Chemistry
- Flavins for Chemical Synthesis
- Flavins in Natural Product Biosynthesis
- Flavins in Signal Transduction
- Fine-tuning Flavin Chemistry
- Flavoprotein Dynamics
- Flavoproteins & Health

This Proceedings book contains articles on subjects presented at the Symposium serving as an update on the field and as a reference manual.

ISBN 978-1-300-78640-5
90000
9 781300 786405

FLAVINS AND FLAVOPROTEINS 2011

EDITORS
S. MILLER
R. HILLE
B. PALFEY

Lulu.com

FLAVINS AND FLAVOPROTEINS 2011

EDITORS
Susan Miller
Russ Hille
Bruce Palfey

Lulu.com

Flavin-Dependent Monooxygenases in Mycobacterial and Fungal Siderophore Biosynthesis

Pablo Sobrado
Dept. of Biochemistry, Virginia Tech, Blacksburg, VA USA

Introduction

Iron is an essential nutrient for bacterial and fungal growth but it is unavailable to invading microbial pathogens in humans, as it is sequestered by iron-binding proteins such as transferrin, lactoferrin, and hemoglobin. To overcome this iron deficiency, pathogenic microbes synthesize and secrete low-molecular-weight iron chelators, called siderophores, to scavenge iron from the host [1]. Siderophores are synthesized via non-ribosomal peptide synthetases and contain functional groups such as carboxylates, catecholates, and hydroxamates, which are essential for iron binding. Hydroxamate functional groups are derived from the hydroxylation of the amino group on the side chains L-lysine or L-ornithine. This reaction is catalyzed by flavin-dependent monooxygenases (Scheme 1) [2,3]. *Mycobacterium smegmatis* G (MbsG), the flavoprotein that catalyzes the hydroxylation of lysine present in the siderophore mycobactin, is essential for mycobacterial survival under iron-limiting conditions [4].

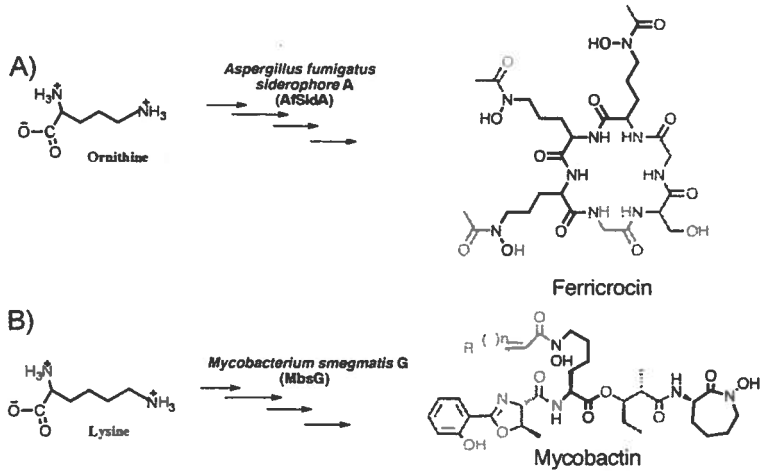

Scheme 1. A) The ferricrocin siderophore of *Aspergillus fumigatus* contains ornithine residues that are hydroxylated by *Af* SidA. B) Mycobactin siderophores contain lysines that are hydroxylated by MbsG.

Thus, it has been proposed that this enzyme is an attractive target for drug design against mycobacteria. Similarly, in *Aspergillus fumigatus*, deletion of the gene coding for the N^5-ornithine hydroxylase (*Af* SidA) involved in ferricrocin biosynthesis results in a mutant strain of *A. fumigatus* that is unable to cause infection in mice, demonstrating that this enzyme is essential for virulence [5]. We have selected *Af* SidA and MbsG because they are the first members of this family of enzymes to be isolated with the flavin bound. Previously, our group and others established that *Af* SidA catalyzes the NADPH and oxygen dependent N^5-ornithine hydroxylation using a sequential kinetic mechanism. In this reaction, $NADP^+$ remains bound and is the last substrate to be released [6,7]. The reduced enzyme-$NADP^+$ complex is capable of stabilizing the C4a-hydroperoxyflavin, which is the hydroxylating intermediate. NADH is also a substrate for *Af* SidA, however, it is 2-fold less effective in stabilizing the hydroxylating flavin intermediate than NADPH. We compared the reactivity of these coenzymes in both the reductive and oxidative half-reactions. Furthermore, we show that there are differences in the function between the eukaryotic (*Aspergillus*) and prokaryotic (*Mycobacterium*) enzymes. In addition, we discuss the design and implementation of a fluorescence polarization binding assay, which can be used for high-throughput screening of small molecule inhibitors that will target siderophore biosynthesis in fungi and mycobacteria.

Materials and Methods

Protein expression, purification, detection of hydrogen peroxide and hydroxylamine, and oxygen consumption assays where performed as previously described [6]. Detection and quantitation of superoxide was done by monitoring the change in absorbance of water-soluble tetrazolium-1 to formazan (ε_{438} = 37,000 M^{-1} cm^{-1}). Changes in the flavin fluorescence (excitation: 450 nm, emission: 520 nm) were recorded on a SpectraMax M5e plate reader (Molecular Devices) and the data analyzed following the procedures of Oppenheimer *et al* [8]. [*4R*-^{2}H]NADPH (NADPD) and [*4R*-^{2}H]NADH (NADD) were prepared with alcohol dehydrogenase from *T. brockii* using 2-propanol-^{2}H8 as substrate, and formate dehydrogenase from *C. boidinii* using deuterated formic acid as substrate, respectively. Control samples of NADPH and NADH were prepared as the deuterated samples. Rapid reaction kinetic experiments were carried out at 15 °C using an SX20 stopped-flow

apparatus (Applied Photophysics, UK) installed inside an anaerobic glove box.

The synthesis of the ADP-TAMRA chromophore was achieved by coupling TAMRA-succinimidyl ester to an ADP-linker conjugate that was synthesized by the coupling reaction of AMP triethylammonium salt with a phosphate precursor containing the linker moiety. The product, ADP-TAMRA chromophore, was isolated from the reaction mixture by HPLC, using a C18 column, and characterized by ^{1}H NMR and high-resolution MS. To assess the effect of conformational changes induced by ligand binding, *Af* SidA (8.73 μM final) was diluted to a final volume of 200 μL with 100 mM HEPES, 125 mM NaCl, pH 7.5 buffer, along with either 5 mM $NAD(P)^+$, or 15 mM ornithine. At specific time intervals, aliquots (15 μL) were removed and immediately heated to 95 °C to stop the reaction. The samples were analyzed on a 12% sodium dodecyl sulfate-polyacrylamide gel electrophoresis (SDS-PAGE).

Results & Discussion

Steady-state kinetic isotope effects (KIE) established that *Af* SidA is stereoselective for the *proR*-hydrogen of either NADH or NADPH. When NADPH is used as substrate, the KIE values are close to 3. When NADH is used as substrate, these values decrease to ~2, Table 1.

Table 1. Steady state kinetic parameters and isotope effects for *Af* SidA

	k_{cat}, min^{-1}	K_M, μM	k_{cat}/K_M, min^{-1} μM^{-1}	$^Dk_{cat}$	$^D(k_{cat}/K_M)$
NADPH	36 ± 1	12 ± 0.9	3.0 ± 0.15	3.1 ± 0.2	2.7 ± 0.2
NADPD	11 ± 0.4	10 ± 0.9	1.10 ± 0.1		
NADH	44 ± 1	100 ± 10	0.43 ± 0.03	2.0 ± 0.1	2.5 ± 0.3
NADD	22 ± 1	130 ± 10	0.17 ± 0.02		

To better understand the reduction steps in *Af* SidA, the KIEs were measured in the stopped-flow spectrophotometer. Reduction of the flavin occurred in two phases with either NADH or NADPH (Figure 1). With NADH, the concentration dependence of both phases could be accurately determined. The fast phase increased as the concentration of NADH increased, reaching a maximum value of 1.55 ± 0.01 s^{-1} and a K_d value of 25 μM. The slow phase rate was 0.09 ± 0.003 s^{-1} and did not change as a function of NADH concentration. Only the fast phase

rate was isotope sensitive, with a KIE value of 4.7 ± 0.04 s^{-1}. This indicates that the fast phase corresponds to flavin reduction. We propose that the second phase corresponds to NAD^+ release. The affinity for NADPH is very high (K_d < 3 μM), preventing accurate measurement of the concentration dependence of the reduction. At saturating concentrations (100 μM NADPH), the rate for the fast and slow phase were 0.66 ± 0.01 s^{-1}, and 0.22 ± 0.001 s^{-1}, respectively. The slow rate of flavin reduction provides an explanation for the different KIE values observed under steady-state conditions. The KIE of flavin reduction with NADPH was determined to be 5.5 ± 0.03 s^{-1} for the fast phase, and 5.3 ± 0.9 s^{-1} for the slow phase. Similar results were observed with a related flavin monooxygenase (FMO) from pig liver. With this enzyme, it was proposed that NADPH reacts with different enzyme forms. We propose that NADPH also reacts with different forms of *Af* SidA; it is clear that this does not occur with NADH.

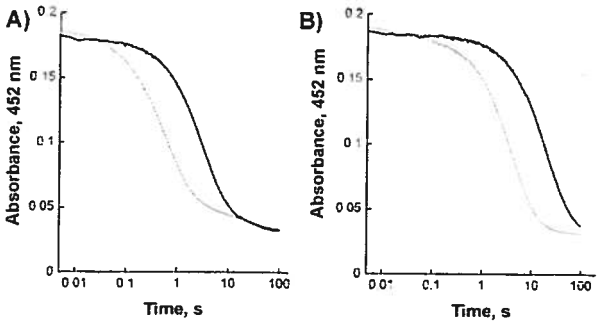

Figure 1. Flavin reduction monitored in the stopped-flow spectrophotometer with NADPH (A) and NADH (B). Reduction with deuterated coenzyme is shown in gray.

The oxidative half-reaction in *Af* SidA was monitored by double-mixing stopped flow experiments where the enzyme was first mixed with equimolar concentrations of NADH or NADPH until full reduction was achieved. The sample was then mixed with oxygenated buffer solution (0.55 mM O_2 after mixing) and different concentrations of ornithine. The formation of the C4a-hydroperoxyflavin was monitored at 362 nm, while the oxidation of the flavin was monitored at 452 nm (Figure 2). The data are summarized in Table 2. The formation of the C4a-hydroperoxyflavin and the oxidized flavin is slightly faster when *Af* SidA is reduced with NADPH. The observed effects must come from the formation of the complex between the

oxidized dinucleotide, oxygenated flavin intermediates, and (hydroxylated)ornithine.

Thus, it appears that $NADP^+$ forms an optimal complex for this half-reaction. This is evident from solvent kinetic isotope effects (SKIE) experiments. In the absence of ornithine, the formation of the C4a-hydroperoxyflavin are partially rate limiting with SKIE values of 1.2 ± 0.1 and 1.3 ± 0.1, for NADPH and NADH, respectively.

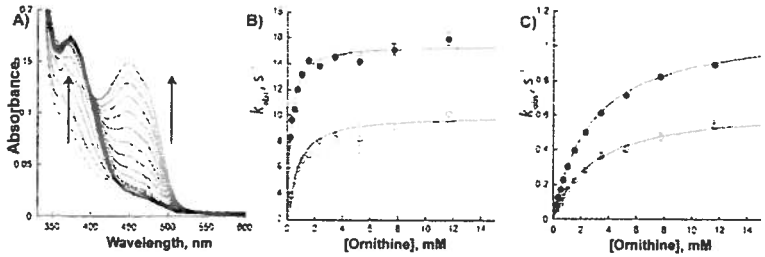

Figure 2. A) Spectral changes during flavin oxidation. B) Dependence of the rate of C4a-hydroperoxyflavin formation on ornithine concentration with *Af* SidA reduced with NADPH (solid circles) or NADH (open circles). C) Same as B but monitoring the formation of the oxidized flavin.

Addition of ornithine, which enhances the rate of formation of this intermediate, results in elimination of the SKIE when the enzyme is reduced with NADPH. In contrast, with NADH, the isotope effect remains the same. The rate of flavin oxidation is the slow step in the oxidative half-reaction. With NADPH, the SKIE value increases to a value close to 2, and is independent of ornithine. In the absence of ornithine, the SKIE value is higher with NADH (2.4 ± 0.1) and increases to 3.6 ± 0.2 in the presence of ornithine.

Table 2. Rate of formation of C4a-hydroperoxy and reduced flavin

Species	coenzyme	$K_{d(app)}$, mM	k_{obs}, s^{-1}
C4a-hydroperoxyflavin	NADPH	0.43 ± 0.03	15 ± 0.2
	NADH	0.53 ± 0.06	10 ± 0.2
Oxidized flavin	NADPH	2.7 ± 0.14	1.1 ± 0.001
	NADH	2.9 ± 0.06	0.65 ± 0.01

These results are consistent with a proton transfer network that is required for catalysis in the oxidative half-reaction in *Af* SidA, which is

optimized when $NADP^+$ is present, while NAD^+ is unable to bind in an optimal position to stabilize the formation of the C4a-hydroperoxyflavin and accelerate the dehydration of the flavin to form the oxidized enzyme for the next catalytic cycle.

Flavin fluorescence as a function of oxidized nucleotide binding provides evidence of a different mode of binding between the two dinucleotides. Binding of NAD^+ results in an increase in the flavin fluorescence (Figure 3A), suggesting that binding of NAD^+ makes the active site environment more hydrophobic.

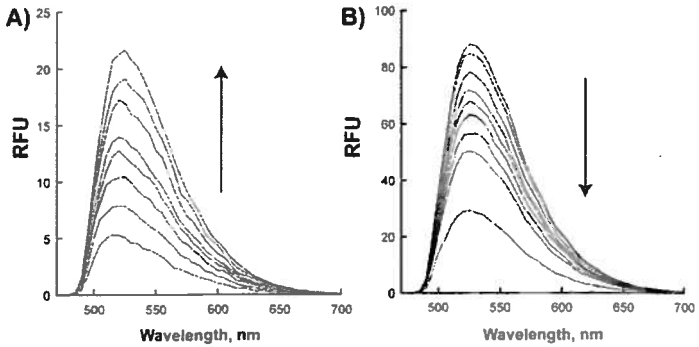

Figure 3. Changes of flavin fluorescence as a function of NAD^+ (A) or $NADP^+$ (B).

Surprisingly, the binding of $NADP^+$ causes the fluorescence of the flavin to decrease (Figure 3B). It appears that $NADP^+$ binds close to the flavin, quenching the fluorescence.

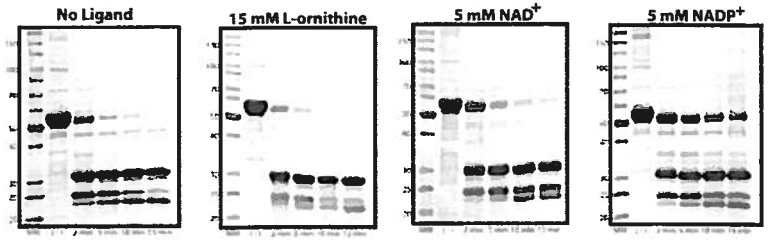

Figure 4. Trypsin digests of *Af* SidA in the presence of various ligands.

Limiting proteolysis studies with *Af* SidA show that binding of $NADP^+$ significantly protects the enzyme from proteolysis by trypsin. This protective effect was not observed with ornithine, and with NAD^+, only a limited protection was detected (Figure 4). Thus, $NADP^+$ specifically modulates enzyme conformational changes in *Af* SidA.

The steady-state kinetic parameters of MbsG with respect to product formation are given in Table 3. MbsG was shown to utilize NADH and NADPH promiscuously; however, a relatively lower K_m value results in 3 fold higher catalytic efficiency for NADH. A decrease in activity was observed at high concentrations of lysine and reduced nucleotide, suggesting substrate inhibition.

The activity of MbsG activity was also monitored by measuring the changes in the concentration of oxygen over time. In the absence of lysine, a much higher k_{cat} value was obtained as compared to the activity measured by directly determining the amount of hydroxylated lysine. Under these conditions, MbsG functions as a flavin oxidase. The k_{cat}/K_m value for NADH is 4 fold higher than for NADPH. This results from a much higher K_m value for NADPH. The apparent higher efficiency with NADH is a unique feature of MbsG.

Table 3. Steady state kinetics of MbsG measuring lysine hydroxylation.

Parameter	NADH	NADPH
k_{cat} (min^{-1})	5.0 ± 0.1	4.6 ± 0.1
$K_{m,\ L\text{-}lys}$ (mM)	0.26 ± 0.02	0.21 ± 0.02
$K_{I,\ L\text{-}lys}$ (mM)	32 ± 4	41 ± 6
$k_{cat}/K_{m,\ L\text{-}lys}$ ($min^{-1}\ mM^{-1}$)	28 ± 6	31 ± 6
$K_{m,\ coenzyme}$ (mM)	1.1 ± 0.2	2.4 ± 0.4
$K_{I,\ coenzyme}$ (mM)	9 ± 2	11 ± 2
$k_{cat}/K_{m,\ coenzyme}$ ($min^{-1}\ mM^{-1}$)	15 ± 4	5 ± 1

Upon the addition of saturating concentration of lysine (3 mM), a lower k_{cat} value is measured. This shows that in the presence of substrate the reaction becomes more coupled and is driven towards product formation (N^6-hydroxy L-lysine). The oxidase activity results in hydrogen peroxide and superoxide (not shown).

Stopped-flow analysis of the reaction between MbsG and reduced dinucleotide were performed under anaerobic conditions in the presence or absence of lysine. The rate of reduction was very close to the rate determined by measuring oxygen consumption. Interestingly,

addition of lysine decreased the rate of flavin reduction in MbsG, Table 4.

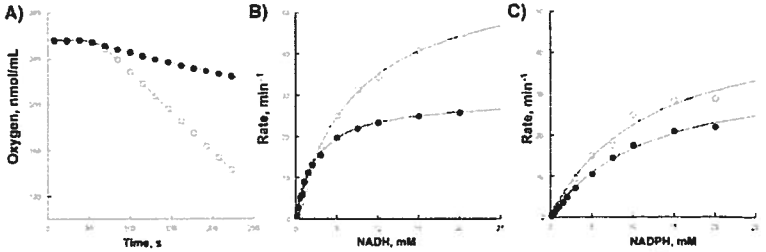

Figure 4. Activity of MbsG measuring oxygen consumption. Panel A shows the traces from the oxygraph instrument. Panel B shows the dependence of the rate as a function of NADH concentration and panel C shows the dependence of the rate as a function of NADPH concentration. In all three panels, open circles represent the absence of lysine, while closed circle represent the presence of lysine (3 mM).

Table 4. Steady-state kinetics of MbsG measuring oxygen consumption and kinetics values measured in the stopped flow.

Parameter	NADH	NADH + Lys	NADPH	NADPH +Lys
k_{cat} (min^{-1})	59 ± 1	29 ± 0.4	32 ± 4	26 ± 2
$K_{m,\,lys}$ (mM)	5 ± 0.2	2.4 ± 0.1	6 ± 1	6 ± 1.4
$k_{cat}/K_{m,lys}$ (min^{-1} mM^{-1})	8.6 ± 0.2	12 ± 0.4	4.3 ± 0.4	5.4 ± 0.6
k_{red} (min^{-1})	59 ± 1	29 ± 0.4	49 ± 3	36 ± 2
$K_{m,\,lys}$ (mM)	5 ± 0.2	2.4 ± 0.1	11 ± 2	14 ± 0.7
$k_{red}/K_{m,\,coenzyme}$ (min^{-1} mM^{-1})	8.6 ± 0.2	12 ± 0.4	4 ± 0.1	3 ± 0.1

N-hydroxylating monooxygenases are important for virulence since their activity is essential for the function of siderophores in *Aspergillus*, *Mycobacterium*, and other human pathogens [4,5]. A fluorescence ligand with high affinity for members of this family of enzymes was designed. The chromophore was built using ADP as a scaffold, since this molecule binds to these enzymes as part of NAD(P)H. We selected the chromophore TAMRA because the excitation and emission wavelength (544 nm and 584 nm, respectively) are different from the flavin and other natural products and will result in low background and

less false positives. For *Af* SidA, a K_d value of 2.0 ± 0.1 μM and for MbsG, a K_d value of 4.0 ± 0.8 were calculated with this chromophore. Using the change in anisotropy upon release of this chromophore from the active site of *Af* SidA, K_d values of 3.7 ± 0.8 μM, 69 ± 17 μM, 4 ± 1.4 mM, and 10 ± 1.3 mM were calculated for $NADP^+$, NAD^+, ornithine, and lysine, respectively. Samples of the competition assays are shown in Figure 5.

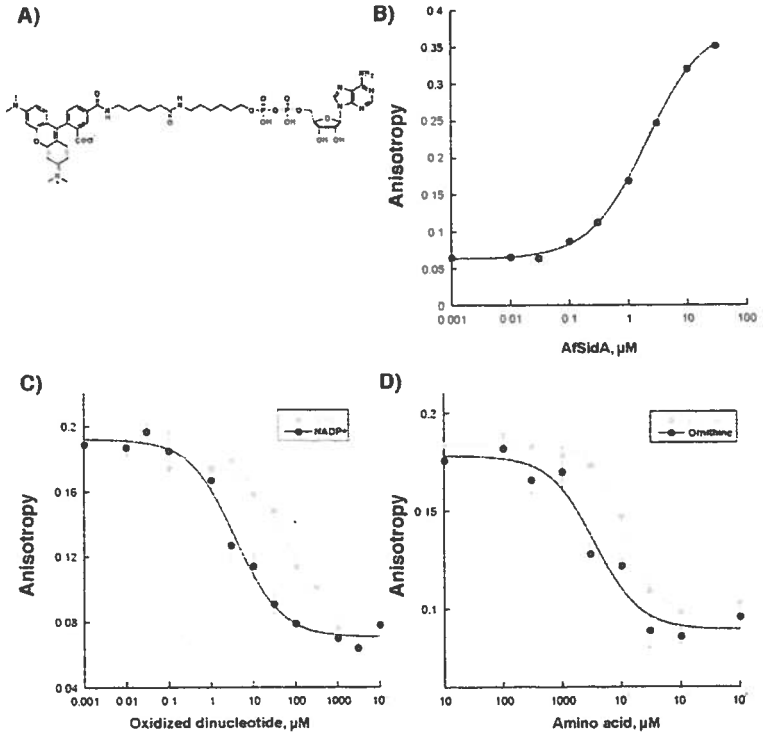

Figure 5. Fluorescence anisotropy-based binding assay for *N*-hydroxylating enzymes. A) Structure of ADP-TAMRA used as reported for ligand binding to *Af* SidA. B) Binding curve of ADP-TAMRA to *Af* SidA. C) Binding of $NADP^+$ and NAD^+ D) Binding of lysine and ornithine.

Conclusions

The mechanism of regulation of *Af* SidA involves the stabilization of the C4a-hydroperoxiflavin to prevent futile utilization of NADPH and the formation of hydrogen peroxide [5,7]. This mechanism is also used by other members of the Class B flavin-dependent monooxygenase

family of enzymes, which includes flavin monooxygenases (FMO) and Baeyer-Villiger monooxygenases (BVMO) [9,10].

The structure of FMO from *Methylophaga sp.* strain SK1 shows that $NADP^+$ is in an incorrect position for hydride transfer; instead, the position was predicted to interact with oxygenated flavin intermediates [9]. It was suggested that domain motions are involved in positioning the nicotinamide ring to perform this role. Structures of cyclohexanone monooxygenase clearly show that such conformational changes occur [10].

The data presented here are consistent with NADP(H) playing a dual role in catalysis--hydride transfer and stabilization of flavin intermediates. We show that after hydride transfer, $NADP^+$ binds in a specific conformation that induces conformational changes. As demonstrated in the related flavin monooxygenases, we propose that these changes are involved in positioning the nicotinamide ring in the correct orientation to interact with the flavin intermediates (Scheme 2). Further evidence comes from the recent elucidation of the 3D-structure of the first ornithine hydroxylase from *Pseudomonas aeruginosa* (PvdA), in complex with $NADP^+$ and ornithine. In this enzyme, the nicotinamide ring is also in a position predicted to interact with the C4a-hydroperoxyflavin [12].

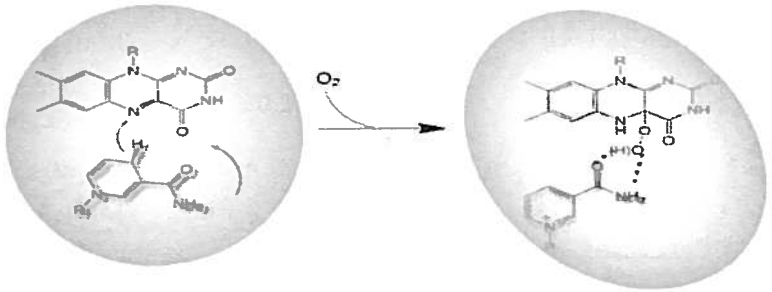

Scheme 2. Cartoon representation of the proposed coenzyme-induced conformational changes in *Af* SidA that lead to the stabilization of oxygenated flavin intermediates. These conformational changes are specific to NADP(H), thus, the 2'-phosphate is involved in this process.

MbsG was shown to hydroxylate free lysine, however, this enzyme has a slight preference for NADH over NADPH and oxidizes these substrates in the absence of lysine, forming hydrogen peroxide and superoxide. Binding of lysine reduces the rate of flavin reduction and makes the enzyme more coupled, forming hydroxylated lysine.

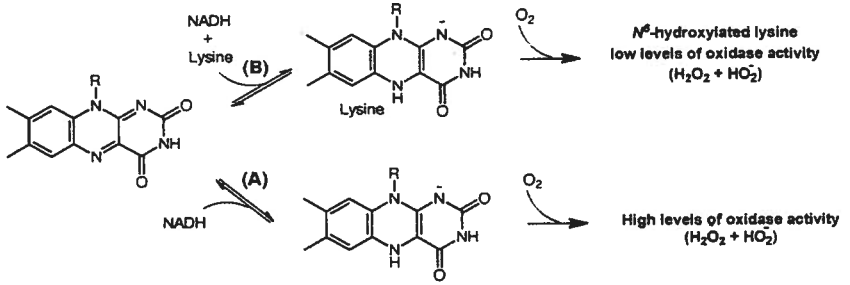

Scheme 3. Substrate regulation mechanism of MbsG. **A)** High levels of oxidase activity observed in the absence of lysine. **B)** In the presence of L-lysine, the oxidase activity of MbsG decreased and the monooxygenase activity increased.

Taking into account the difference in the affinities of MbsG for lysine (~200 μM) compared to NADH (~2 mM), we proposed that in the cell, MbsG is present in complex with lysine, ensuring that upon reaction with NADH productive catalysis will occur (Scheme 3). Further experiments are underway to determine the kinetic mechanism of this interesting enzyme.

By using ADP as the building block for a fluorescent ligand, we developed a compound that binds to both *Af* SidA and MbsG with high affinity. Because the large differences in the molecular weight between the bound enzyme and the free chromophore, large changes in anisotropy can be measured when the chromophore is displaced by molecules that bind in the active site of these enzymes. We tested $NAD(P)^+$, ADP, ornithine, and lysine and demonstrate that these compounds effectively compete for binding with the chromophore, demonstrating that the chromophore is binding at the active site. Furthermore, the calculated K_d values for these molecules are similar to the values determined by other methods. This assay can be used to screen small molecule libraries to find inhibitors against *N*-hydroxylated enzymes. It is possible that this assay can be used for other flavin monooxygenases.

References

1. Fischbach, M. A., Lin, H., Liu, D. R., and Walsh, C. T. (2006) How pathogenic bacteria evade mammalian sabotage in the battle for iron. *Nat. Chem. Biol.* **2**, 132-138.
2. Quadri, L. E., Sello, J., Keating, T. A., Weinreb, P. H., and Walsh, C. T. (1998) Identification of a Mycobacterium tuberculosis gene cluster encoding the biosynthetic enzymes for assembly of the

virulence-conferring siderophore mycobactin. *Chem. Biol.* **5**, 631-645.

3. van Berkel, W. J., Kamerbeek, N. M., and Fraaije, M. W. (2006) Flavoprotein monooxygenases, a diverse class of oxidative biocatalysts. *J. Biotechnol.* **124**, 670-689.
4. Sassetti, C. M., Boyd, D. H., and Rubin, E. J. (2003) Genes required for mycobacterial growth defined by high density mutagenesis. *Molecular Microbiology* **48**, 77-84.
5. Hissen, A. H., Wan, A. N., Warwas, M. L., Pinto, L. J., and Moore, M. M. (2005) The Aspergillus fumigatus siderophore biosynthetic gene sidA, encoding L-ornithine N5-oxygenase, is required for virulence. *Infect. Immun.* **73**, 5493-5503.
6. Chocklett, W.S, Sobrado, P. (2010) *Aspergillus fumigatus* SidA is a highly specific ornithine hydroxylase with bound flavin cofactor. *Biochemistry* **49**, 6777-6783
7. Mayfield, JA, Frederick, R.E., Streit, B.R., Wencewicz, T.A., Ballou, D.P., Dubois, J.L. (2010) Comprehensive spectroscopic, steady state, and transient kinetic studies of a representative siderophore-associated flavin monooxygenase. *J. Biol. Chem.* **285**, 30375-30388
8. Oppenheimer, M, Poulin MB, Lowary TL, Helm RF, Sobrado P. (2010) Characterization of UDP-Galactopyranose mutase from *Aspergillus fumigatus*. *Arch. Biochem. Biophys.* **502**, 31–38
9. Alfieri, A., Malito, E., Orru, R., Fraaije, M. W., and Mattevi, A. (2008) Revealing the moonlighting role of NADP in the structure of a flavin-containing monooxygenase. *Proc. Natl. Acad. Sci. (U S A)* **105**, 6572-6577.
10. Mirza IA, Yachnin BJ, Wang S, Grosse S, Bergeron H, Imura A, Iwaki H, Hasegawa Y, Lau PC, Berghuis AM. (2009) Crystal structures of cyclohexanone monooxygenase reveal complex domain movements and a sliding cofactor. *J. Am. Chem. Soc.* **131**, 8848-8854.
11. Van Berkel, W.JH., Kamerbeek, N.M., Fraaije, M.W. (2006) Flavoprotein monooxygenases, a diverse class of oxidative biocatalysts. *J. Biotech.* **124**, 670-689.
12. Olucha J, Meneely KM, Chilton AS, Lamb AL. Olucha J, Meneely KM, Chilton AS, Lamb AL. (2011) Two structures of an *N*-hydroxylating flavoprotein monooxgenase: the ornithine hydroxylase from *Pseudomonas aeruginosa*. *J. Biol. Chem.* **286**, 31789-31798.

Flavins on the Move: Flavoprotein Hydroxylases and Epoxidases

Willem J. H. van Berkel[1], Stefania Montersino[1], Dirk Tischler[2], Stefan Kaschabek[2], Michael Schlömann[2], George T. Gassner[3]

[1]Laboratory of Biochemistry, Wageningen University, Wageningen, The Netherlands

[2]Environmental Microbiology, TU Bergakademie Freiberg, Germany

[3]Department of Chemistry and Biochemistry, San Francisco State University, San Francisco, USA

Introduction

Flavoprotein monooxygenases perform chemo-, regio- and/or enantioselective oxygenations of organic substrates under mild reaction conditions [1]. These properties along with effective preparation methods make flavoprotein monooxygenases a focus of industrial biocatalysis. Here we describe two biocatalytically relevant subclasses of flavoprotein monooxygenases with a close evolutionary relation: class A represented by *p*-hydroxybenzoate hydroxylase (PHBH) and class E formed by styrene monooxygenases (SMOs).

PHBH family members perform highly regioselective hydroxylations on a wide variety of aromatic compounds. A rapid increase in available crystal structures and detailed mechanistic studies of such enzymes [2] are opening a new season of research in the field.

SMOs catalyze a number of stereoselective epoxidation and sulfoxidation reactions [3]. Mechanistic and structural studies expose distinct characteristics, which provide a promising source for future biocatalyst development [4]. Nearly all bacterial SMOs are two-component proteins comprising a reductase and a monooxygenase. Remarkably, in a few cases, the reductase is fused to the monooxygenase [5]. Such a self-sufficient enzyme can also cooperate with a single monooxygenase, resulting in a novel type of two-component SMO [6].

Results & Discussion

Flavoprotein monooxygenases can be divided in six different subclasses based on structural features and oxygenation chemistry [1]. Table 1 gives an overview of the crystal structures of single-component flavoprotein aromatic hydroxylases (class A) and two-component